

Bimetallic Pt and Ni Based Foam Catalysts for Low-Temperature Ethanol Steam Reforming Intensification

Vincenzo Palma, Concetta Ruocco, Antonio Ricca*

University of Salerno, D. I. In., Via Giovanni Paolo II 132, 84084 Fisciano (SA), Italy
 aricca@unisa.it

The increasing world power demand is driving scientific interest toward the research of alternative energy sources. As energy production from fossil fuels is limited by both reduced availability and pollutants emissions, H₂ from renewable feed-stocks (i.e. bioethanol) appears a good clean chance, especially for fuel cells. In this paper, the performances of ceria and ceria-zirconia supported bimetallic powder and foam catalysts in the low temperature range (300-600 °C) Ethanol Steam Reforming reaction were investigated with the aim to highlight the improved heat transfer properties of the structured samples. Two different reactor configurations were employed: catalytic powders were tested in both an annular and a tubular reactor and the hollow one was also used for foam catalysts. SiC foam catalysts, by exploiting the high thermal conductivity of the support, could reduce heat transfer resistance, thus assuring very interesting results in terms of both activity and stability. Moreover, the role of catalytic support was studied and CeO₂-ZrO₂ based catalysts were found more suitable for the desired reaction.

1. Introduction

The search for alternative energy sources, looking towards the reduction of pollutants and greenhouse gases, increases more and more and hydrogen is often suggested as a very promising energetic vector (McDowall et al., 2007). This attractive fuel, in fact, can be directly converted in electrical power through fuel cell technology with pure water as the only by-product. In this way, environmental benign energy production is allowed. However, the non-polluting character of the whole process is strongly affected by the H₂ source employed. Despite the most widespread H₂ production technologies involve hydrocarbon steam reforming (Koroneos et al., 2004), clean energy supply can be provided only by making hydrogen from renewable feed-stocks. Among them, biomass, cheap and carbon neutral resource, looks as one of the most viable candidates. From the fermentation of sugar, starch and cellulose, bioethanol can be derived which becomes, in turn, an interesting H₂ source. As bioethanol mixtures contain much water, its reforming with steam (Eq(1)) appears one of the best obvious method to recover hydrogen (Ni et al., 2007).



Due to steam reforming endothermicity, high temperatures are required to increase H₂ yield. However, in order to minimize carbon monoxide (CO) formation and heat duty, lower temperatures may be selected. In these operating conditions, carbonaceous deposits are thermodynamically favoured (Mas et al., 2006) and side reactions can negatively affect H₂ selectivity. Therefore, the proper choice of active towards the desired reaction and coke resistant catalysts was the focus of many studies. Ethanol Steam Reforming (ESR) was investigated over both non-noble (Ni, Co, Cu) and noble metals (Pt, Rh, Ru, Pd) also by highlighting the role of catalytic support. When Al₂O₃ is employed, ethanol dehydrogenation reaction to ethylene is responsible for coke formation and catalyst deactivation (Batista et al., 2004). Conversely, rare earth oxides, such as CeO₂ and CeO₂-ZrO₂, due to their well-known oxygen storage capacity (OSC), promote carbon gasification and prevent sintering phenomena (de Lima et al., 2008). Despite the interesting performances of monometallic catalysts, bimetallic ones, which take advantages from the synergistic effect of both metals, were also studied

due to their improved activity and stability (Men et al., 2007). Bimetallic Pt-Ni/CeO₂ powder catalyst ensured a good agreement of product distribution with the thermodynamic data even at low T (Palma et al., 2014). However the heat transfer issue, typical of reforming reactions and very tricky for packed beds, raises the interest toward the development of high thermal conductivity structured catalysts (Palma et al., 2013).

This work is aimed at comparing the catalytic performances of bimetallic Pt-Ni powders and silicon carbide (SiC) coated foams for low-temperature ESR (300-600 °C) at very high space velocities (100,000 - 400,000 h⁻¹). Moreover, the effect of support (CeO₂ and CeO₂-ZrO₂) on activity and stability was also investigated.

2. Experimental

2.1 Catalyst preparation and characterization

Catalysts (3 wt% Pt-10 wt% Ni over CeO₂ and CeO₂-ZrO₂) were prepared by wet impregnation.

The powders preparation started with the addition of calcined support (ceria or ceria-zirconia) to an aqueous solution of the salt precursors (nickel acetate for Ni and platinum chloride for Pt, both from Aldrich). After the impregnation, the samples were dried overnight and calcined at 600 °C for 3 h. Two following impregnations were performed and Ni was deposited on support surface earlier than Pt. The role of impregnation order on catalyst activity was previously studied and the impregnation order optimized (Palma et al., 2012).

SiC cylindrical foams (30 ppi, D14.2 x 21.1 mm) were supplied by IKTS of Dresda, where washcoat deposition procedure was also developed. Conversely, the active species deposition was carried out at University of Salerno; the same impregnation order described for powders was followed. After impregnation, CeO₂ and CeO₂-ZrO₂ (170.9 g/L) based foams were dried for 2 h and calcined for 1 h at a temperature selected on the basis of salt thermo-gravimetric analysis, not reported, and equal to 450 °C and 550 °C, respectively for nickel acetate and platinum chloride. The whole procedure was repeated up to reach the desired metals loading. A further calcination at 600 °C for 3 h was performed in order to stabilize the catalyst. The final catalyst amounts (active species + catalytic support) were 0.789 g for CeO₂ and 0.548 g for CeO₂-ZrO₂.

The prepared samples were characterized through different techniques. Specific area measurements were carried out through N₂ adsorption at -196 °C, using a Sorptometer 1040 "Kelvin" from Costech Analytical Technologies. X-ray diffraction spectra were produced by a D8 Brooker and average crystallites size was calculated by means of Scherrer formula. The reduction behaviour of Pt and Ni species was investigated through temperature programmed reduction (TPR), (0-600 °C at 20 °C/min + 1 h at 600 °C) in the laboratory apparatus described in the next section and by feeding a 5 %H₂ in N₂ stream (GHSV = 114,350 h⁻¹).

2.2 Catalyst testing

ESR was performed in the laboratory apparatus previously reported (Palma et al., 2012). Powders (180-355 µm), sandwiched between two quartz flakes, were tested in both an annular and a tubular reactor and the hollow configuration was also employed for foams, held in place by means of a ceramic pad. The reactor was paced in an electrical oven and the catalytic volume temperature was monitored at the center of the catalyst end section. After H₂ reduction in situ, water/ethanol mixture, stored in a tank pressurized by nitrogen, was fed to the reaction section by means of a mass flow controller for liquid (Quantim by Brooks). Before reaching the reactor, the liquid mixture was diluted with N₂ and then vaporized in a boiler. Two four way Nupro valves allowed the reaction mixture to be send to the reactor or, alternatively, to the analysis section. Traced lines (140 °C) were used in components linking to avoid condensation. The product gas composition was continuously monitored by means of FT-IR spectrophotometer (Nicolet Antaris IGS by Thermo Electron). As diatomic molecules do not adsorb infrared radiation, a thermo-conductivity analyzer (CALDOS 27 by ABB) was employed to record H₂ concentration. A sample gas conditioning system, placed between the analyzers, ensured ABB normal operation. ESR tests were carried out at atmospheric pressure and at temperature ranging between 300 and 600 °C. The reaction flow-rate (5 % C₂H₅OH, 15 % H₂O and 80 % N₂) was selected to assure a gas hourly space velocities (GHSV) varying from 100,000 to 400,000 h⁻¹. The same catalytic mass deposited on foams (0.789 g for CeO₂ and 0.548 g for CeO₂-ZrO₂) was employed for powders tests; in order to reduce pressure drops through the bed, powders samples were diluted with quartz (1:1 vol, 500-710 µm).

3. Results and discussion

3.1 Supports and catalysts characterization

The results of BET and XRD analyses were summarized in Table 1. A reduction of the surface area can be observed for both CeO₂ and CeO₂-ZrO₂ based samples after Ni and Pt deposition. This specific surface area (SSA) loss is ascribable to the plugging of some support pores occurring during preparation. Despite ceria-zirconia SSA was lower than ceria, a more significant area reduction was recorded for Pt-Ni/CeO₂ catalyst.

Table 1: Textural properties and particles size of supports and active species

| Sample | SSA (m ² /g) | Support <i>d</i> (Å) | NiO <i>d</i> (Å) |
|--|-------------------------|----------------------|------------------|
| CeO ₂ | 127 | 55 | - |
| Pt-Ni/CeO ₂ | 72 | 70 | 105 |
| CeO ₂ -ZrO ₂ | 64 | 69 | - |
| Pt-Ni/CeO ₂ -ZrO ₂ | 49 | 73 | 166 |

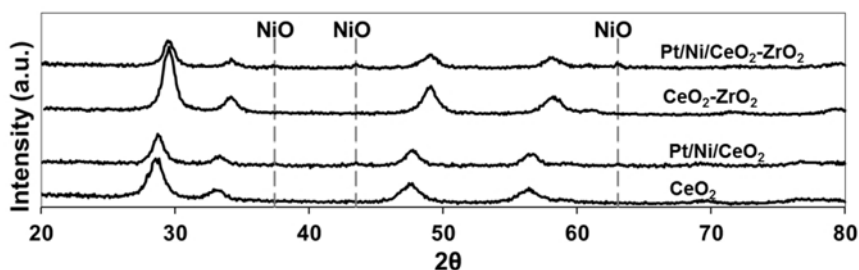
Figure 1: XRD spectra of CeO₂, CeO₂-ZrO₂ and Pt-Ni based samples

Figure 1 shows the X-ray diffraction patterns of supports and bimetallic catalysts. Calcined ceria sample is composed of cubic CeO₂ with fluorite structure. For CeO₂-ZrO₂ support, the substitution of cerium with zirconium, according to the lower ionic radius of Zr⁴⁺ with respect to Ce⁴⁺, caused a ceria XRD peaks shift to larger 2θ values (Escribano et al., 2003). Characteristic diffraction lines at 37.265, 43.298 and 62.896 ° of NiO (ICDD file: 78-0643) were visible in the spectrum of Pt-Ni samples while there was no evidence of the peaks corresponding to Pt species, thus indicating mean PtO₂ diameters less than 5nm. The crystallites size (*d*) of CeO₂, CeO₂-ZrO₂ and NiO were evaluated from Scherrer relation. A support grains dimension increase as a consequence of metals impregnation and higher dispersion of NiO on CeO₂ with respect to CeO₂-ZrO₂ one were observed. This lower NiO crystallites size may be linked to the high SSA of ceria (Fajardo et al., 2010). The deconvoluted reduction profiles of Pt-Ni based catalysts are reported in Figure 2 while the calculated hydrogen consumptions are compared with the theoretical ones in Table 2.

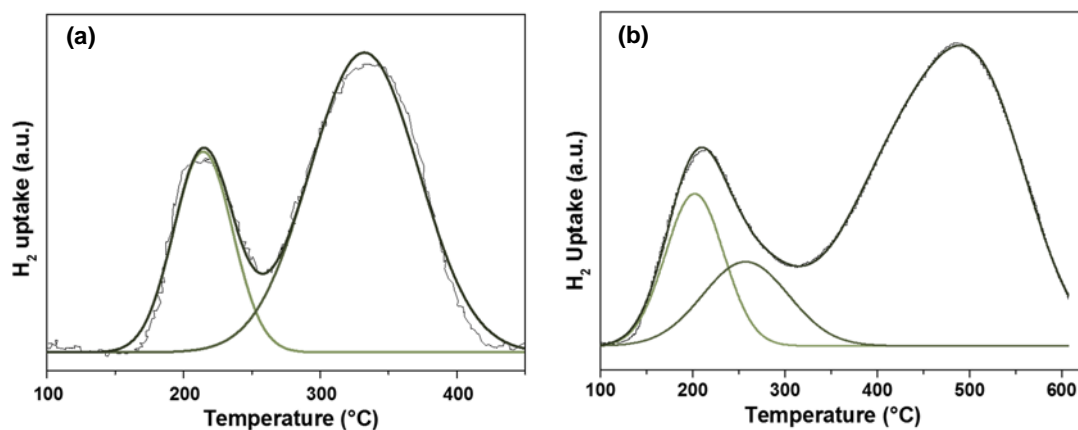
Figure 2: TPR profiles of Pt-Ni/CeO₂ (a) and Pt-Ni/CeO₂-ZrO₂ catalysts (b)

Table 2: Hydrogen consumption for bimetallic catalysts

| Sample | Active species oxide | Peak position (°C) | Theoretical (μmol/g) | Experimental (μmol/g) |
|--|----------------------|--------------------|----------------------|-----------------------|
| Pt-Ni/CeO ₂ | PtO ₂ | 214 | 308 | 624 |
| | NiO | 332 | 1,704 | 1,710 |
| Pt-Ni/CeO ₂ -ZrO ₂ | PtO ₂ | 202 | 308 | 2,336 |
| | NiO | 257 | 1,704 | 1,898 |

The lower temperature peak (*T* = 214 °C) observed in the TPR results of Pt-Ni/CeO₂ sample (Figure 2 a) is assigned to the reduction of PtO₂ while the peak at 332 °C can be related to NiO reduction. The H₂ uptake

ascribable to PtO₂, as a consequence of H₂ spillover phenomena promoted in the presence of the noble metal (Laguna et al., 2011), is almost twice (624 $\mu\text{molH}_2/\text{g}_{\text{cat}}$) the expected one; no difference were observed between experimental and theoretical uptakes in the case of NiO. The TPR profile recorded on Pt-Ni/CeO₂-ZrO₂ catalyst (Figure 2 b) showed lower reduction temperatures with respect to what observed for CeO₂ based sample and equal, respectively, to 202 °C and 257 °C for PtO₂ and NiO. In fact, ZrO₂ incorporation in ceria lattice enhances Ce⁴⁺ reducibility (Saidina et al., 2005), thus shifting reduction peaks leftward. Moreover, the H₂ consumption between 120 °C and 250 °C reached 2,336 $\mu\text{molH}_2/\text{g}_{\text{cat}}$, which means one order of magnitude higher than the theoretical one. The significant influence of H₂ spillover, observed when Pt is supported on ceria-zirconia, well agrees with data reported in the literature (Takeguchi et al., 2001).

3.2 Catalytic behavior of Pt-Ni/CeO₂ and Pt-Ni/CeO₂-ZrO₂

The activity of CeO₂ based powders and foams for ESR was preliminary tested by evaluating ethanol conversion (Figure 3 a) and hydrogen yield (Figure 3 b) as a function of the reaction temperature. The Pt-Ni/CeO₂ powder tested in the annular configuration, despite the very low contact time, showed an interesting catalytic performance, ensuring total C₂H₅OH conversion at T > 500 °C (Figure 3a); a good agreement, in terms of H₂ yield, between experimental values and thermodynamic predictions was also ensured. The same catalyst, tested in the tubular reactor, exhibited lower activity and, as a consequence, no satisfactory ethanol conversions were recorded even at high temperatures. The annular configuration, in fact, involves very low resistance to heat transfer between the heating medium and catalytic volume, thus resulting in an easier reaction control (Marigliano et al., 2001). On the contrary, the pronounced deviation of thermal radial profile from linearity, caused by the lower heat fluxes, was responsible for the worst performance observed when the powder sample was tested in the tubular configuration. A very interesting catalytic behavior was also observed in the case of bimetallic foam catalyst, able to ensure total ethanol conversion to 360 °C. Moreover, H₂ yield profile was very close to the one observed for powder sample tested in the annular reactor (Figure 3 b).

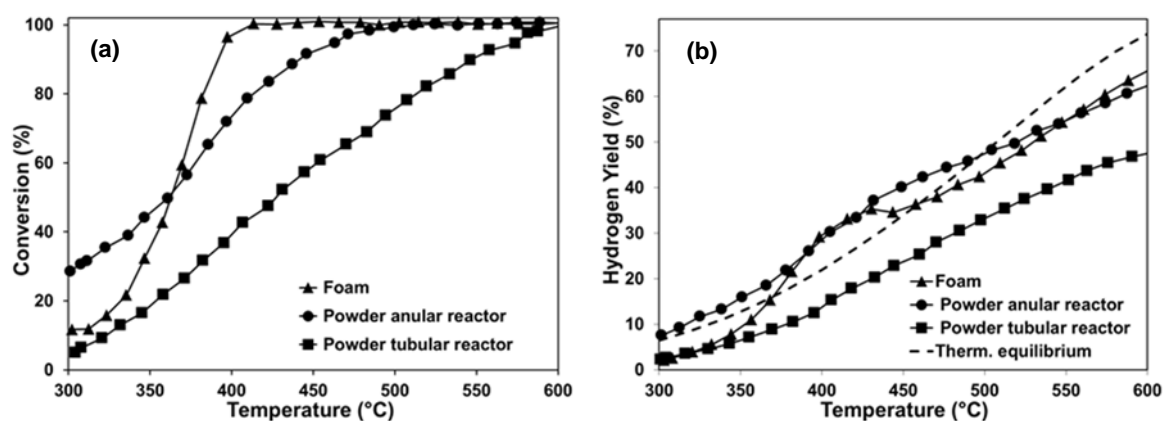


Figure 3: C₂H₅OH conversion (a) and H₂ yield (b) as a function of temperature for Pt-Ni/CeO₂ catalysts; GHSV = 114,350 h⁻¹

The high thermal conductivity of SiC, in fact, increases heat transfer through the catalytic bed; in addition, the foam geometry, able to impose a chaotic flux to the gaseous stream, assures more uniform thermal and composition profiles (Palma et al., 2013). Taking into account the significantly less performance achieved by powder tested in the tubular reactor, further studies were focused on the two most promising systems.

The nature of support also plays a key role in determining activity and selectivity of the final catalyst. Therefore, in order to select the best performing catalyst for ethanol steam reforming, CeO₂-ZrO₂ based powders and foams were also prepared and their catalytic behavior was evaluated in comparison with Pt-Ni/CeO₂ samples. C₂H₅OH concentration increase with reducing temperature and total alcohol conversion was observed at T > 500 °C over all the tested samples (Figure 4a). However, Pt-Ni/CeO₂-ZrO₂ catalysts (powder and foam) were shown to be much more efficient for the desired reaction, allowing a stronger resistance to deactivation at low T. In fact, the higher mobility of ceria-zirconia -OH groups with respect to ceria alone, ensured in optimized solid solutions, as in the present study, in terms of Ce/Zr molar ratios (Aneggi et al., 2006), makes easy oxidation reactions, in particular water gas shift (WGS) and coke gasification. These improved properties resulted in higher H₂ yields (Figure 4 b) and a weaker Pt-Ni/CeO₂-ZrO₂ catalysts deactivation at T < 400 °C. In order to properly evaluate the stability of ceria-zirconia samples, time-on-stream

tests (TOS) were also performed at 450 °C and GHSV = 114,350 h⁻¹; the results (Figure 5) were reported in terms of product gas distribution as a function of time and compared with the equilibrium data.

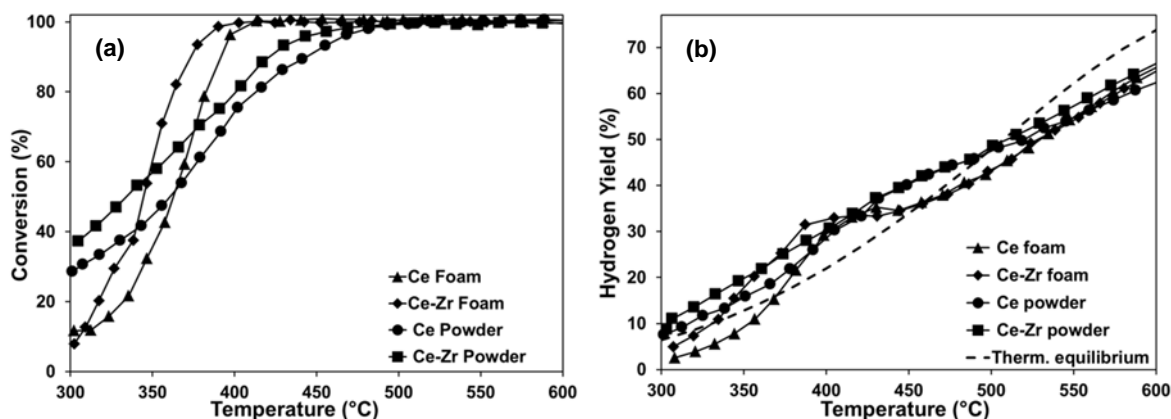


Figure 4: C₂H₅OH conversion (a) and H₂ yield (b) as a function of temperature for Pt-Ni catalysts supported over CeO₂ and CeO₂-ZrO₂; GHSV = 114,350 h⁻¹

Both the foam and powder samples ensured total ethanol conversion for more than 300 min and product distribution was not affected during time-on-stream tests. In particular, a slightly increase in WGS activity was recorded in the case of ceria-zirconia foam, thus resulting in a reduced CO formation (Figure 5 a). Conversely, a higher promotion of reforming reactions was observed over Pt-Ni/CeO₂-ZrO₂ powder, which exhibited H₂O and CO₂ concentrations respectively higher and lower than the thermodynamic predictions (Figure 5 b).

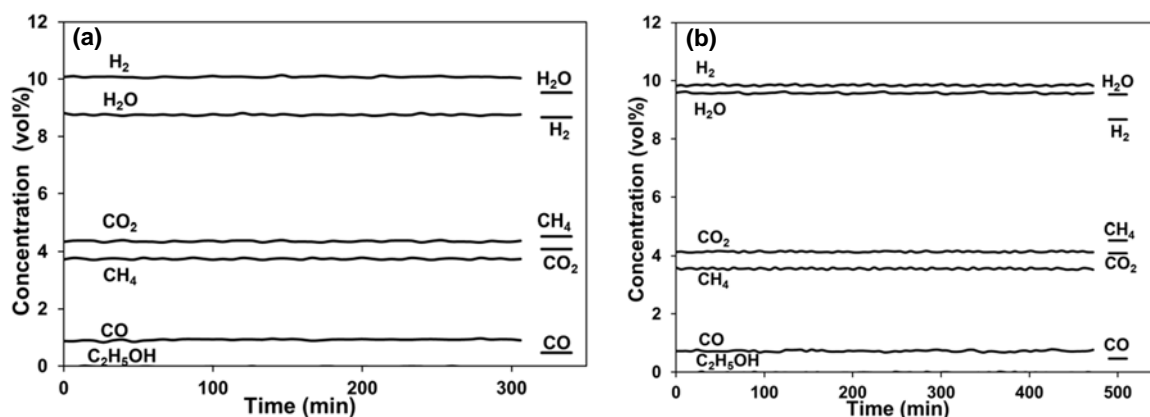


Figure 5: Product gas distribution during TOS tests over (a) CeO₂-ZrO₂ based foam and (b) powder; T = 450 °C, GHSV = 114,350 h⁻¹

Table 3: Results of catalytic tests performed at 450 °C over Pt-Ni/CeO₂-ZrO₂ catalysts

| Sample | GHSV [h ⁻¹] | X (%) | Y (%) | T ₀ (°C) |
|--------|-------------------------|-------|-------|---------------------|
| Foam | 100,000 | 100 | 35.1 | 471 |
| | 200,000 | 100 | 34.8 | 471 |
| | 400,000 | 99.9 | 34.6 | 472 |
| Powder | 100,000 | 100 | 39.1 | 479 |
| | 200,000 | 99.9 | 39.1 | 480 |
| | 400,000 | 99.9 | 38.6 | 482 |

The effect of space velocity on the catalytic behavior of Pt-Ni/CeO₂-ZrO₂ catalysts at 450 °C was also investigated and the results, reported in terms of C₂H₅OH conversion (X) and H₂ yield (Y), are summarized in Table 3. The catalysts activity was not affected by contact time decrease; moreover, despite fairly stable H₂ yields were observed over both the samples, CeO₂-ZrO₂ powder showed higher production of the desired gas.

During these tests, the oven temperatures (T_o) to be fixed in order to reach the desired 450 °C within the catalytic bed were also monitored (last column, Table 3). In the case of the structured catalyst, lower temperatures were required, thus demonstrating the reduced resistance to heat transfer in foams. Furthermore, these values, as a consequence of the more uniform temperature profile achievable with respect to powders, were less influenced by space velocity increasing.

The employment of an easier reactor configuration (i.e. tubular), allowed by the structured catalysts, and the way of reducing heat transfer medium temperature may positively impact on plant capital and operating costs.

4. Conclusions

In the present study, the activity and stability of bimetallic powder and structured catalysts were investigated by evaluating the effect of support (CeO_2 and $\text{CeO}_2\text{-ZrO}_2$) and reactor configuration (annular and tubular) on low-temperature ESR performances. The more uniform temperature profile in radial direction, assured by the annular reactor, was responsible for a very interesting catalytic behavior of powder samples; the same catalyst, tested in the tubular configuration, reached less promising results, due to the more difficult thermal management within the catalytic bed. Foams in the tubular reactor showed $\text{C}_2\text{H}_5\text{OH}$ conversions and H_2 yields very similar to the ones exhibited by powders in the annular reactor. In fact, the special thermal conductivity of SiC coupled with the high transfer rates of foams allowed the reduction of thermal resistance typical of tubular reactor. Therefore, in a process intensification view, catalytic foams appear very attractive, due to the high performances reached in a cheaper reactor (i.e. tubular) and the lower costs required for heating.

Finally, from the comparison between ceria and ceria-zirconia based catalysts, it was clear that a better OSC, achievable with proper Ce/Zr ratios, can assure higher activity and stability even at very low contact time.

References

- Aneggi E., Boaro M., de Leitenburg C., Dolcetti G., Trovarelli A., 2006, Insights into the redox properties of ceria-based oxides and their implications in catalysis, *J. Alloy Compd.*, 408–412 1096–1102.
- Batista M.S., Santos R. K.S, Assaf E.M., Assaf J.M., Ticianelli E. A., 2004, High efficiency steam reforming of ethanol by cobalt-based catalysts, *J. Power Sources*, 134, 27–32.
- de Lima S.M., da Cruz I.O., Jacobs G., Mattos L. V., Noronha F. B., 2008, Steam reforming, partial oxidation, and oxidative steam reforming of ethanol over Pt/CeZrO₂ catalyst, *J. Catal.*, 257, 356–368.
- Escribano V. S., López E. F., Panizza M., Busca G., 2003, Characterization of cubic ceria–zirconia powders by X-ray diffraction and vibrational and electronic spectroscopy, *Solid State Sci.*, 5, 1369–1376.
- Fajardo H. V., Longo E., Mezalira D. Z., Nuernberg G. B., 2010, Influence of support on catalytic behavior of nickel catalysts in the steam reforming of ethanol for hydrogen production, *Environ. Chem. Lett.*, 8, 79–85.
- Koroneos C, Dompros A., Roumbas G., Moussiopoulos N., 2004, Life cycle assessment of hydrogen fuel production processes, *Int. J Hydrogen Energ.*, 29, 1443–1450.
- Laguna O.H., Centeno M.A., Romero-Sarria F., Odriozola J.A., 2011, Oxidation of CO over gold supported on Zn-modified ceria catalysts, *Catal. Today*, 172, 118– 123.
- Marigliano G., Barbieri G., Drioli E., 2001, Effect of energy transport on a palladium-based membrane reactor for methane steam reforming process, *Catal. Today*, 67, 85–99.
- Mas V., Kipreos R., Amadeo N., Laborde M., 2006, Thermodynamic analysis of ethanol/water system with the stoichiometric method, *Int. J Hydrogen Energ.*, 31, 21–28.
- Men Y., Kolb G., Zapf R., Hessel V., Loewe H., 2007, Ethanol Steam Reforming in a Microchannel Reactor, *Process Saf. Environ.*, 85, 413–418.
- McDowall W., Eames M., 2007, Towards a sustainable hydrogen economy: A multi-criteria sustainability appraisal of competing hydrogen futures, *Int. J. Hydrogen Energ.*, 32, 4611–4622.
- Ni M., Leung D.Y.C., Leung M.K.H., 2007, A review on reforming bio-ethanol for hydrogen production, *Int. J. Hydrogen Energ.*, 32, 3238–3247.
- Palma V., Castaldo F., Ciambelli P., laquaniello G., 2012, Bio-ethanol steam reforming reaction over bimetallic ceria-supported catalysts. *Chem. Eng. Trans.*, 29, 109–114, DOI: 10.3303/CET1229019.
- Palma V., Ricca A., Ciambelli P., 2013, Methane auto-thermal reforming on honeycomb and foam structured catalysts: The role of the support on system performances, *Catal. Today*, 216, 30– 37
- Palma V., Castaldo F., Ciambelli P., laquaniello G., 2014, CeO₂-supported Pt/Ni catalyst for the renewable and clean H₂ production via ethanol steam reforming, *Appl. Catal. B-Environ.*, 145, 73–84.
- Saidina Amin N.A., Chong C.M., 2005, SCR of NO with C₃H₆ in the presence of excess O₂ over Cu/Ag/CeO₂-ZrO₂ catalyst, *Chem. Eng. J.*, 113, 13–25.
- Takeguchi T., Furukawa S., Inoue M., 2001, H₂ Spillover from NiO to the Large Surface Area CeO₂-ZrO₂ Solid Solutions and Activity of the NiO/CeO₂-ZrO₂ Catalysts for POX of Methane, *J. Catal.* 202 14–24.